

## Redox-Assisted Asymmetric Ostwald Ripening of CdSe Dots to Rods

Rongfu Li,<sup>†</sup> Zhengtang Luo,<sup>†</sup> and Fotios Papadimitrakopoulos<sup>\*,†,‡</sup>

*Nanomaterials Optoelectronics Laboratory, Polymer Program, Institute of Materials Science, and  
Department of Chemistry, University of Connecticut, Storrs, Connecticut 06269-3136*

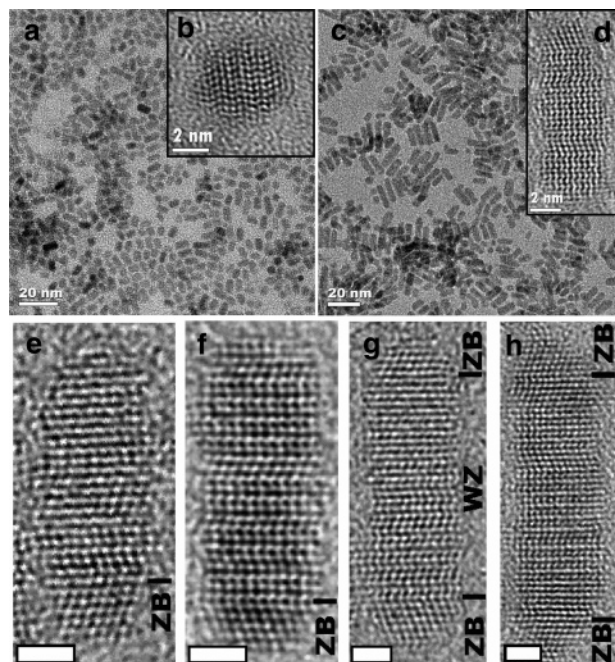
Received November 29, 2005; E-mail: papadim@mail.ims.uconn.edu

The size- and shape-dependent optical and electronic properties of semiconductor nanocrystals (NCs) have attracted considerable attention in recent years.<sup>1</sup> Application-specific usage of these NCs has intensified research toward controlling their shape.<sup>2,3</sup> The linearly polarized emission and larger Stokes shift of CdSe nanorods are of significant interest as well.<sup>4</sup> These rods are typically synthesized through kinetically controlled processes by carefully adjusting the concentration of precursor and capping agents.<sup>5–7</sup> In this Communication, we report our initial findings of the formation of CdSe nanorods via a redox-assisted asymmetric Ostwald ripening from dots to rods.

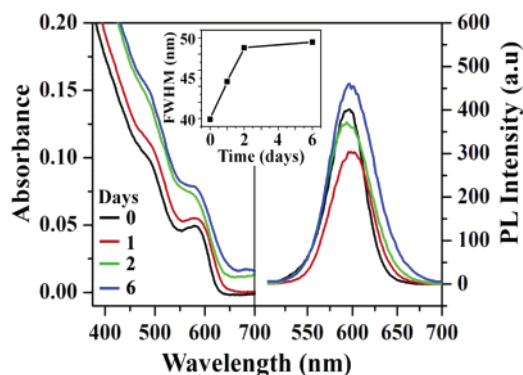
As part of our amine-induced etching investigation of CdSe NCs,<sup>8,9</sup> we presently show that, under certain conditions, NCs grow asymmetrically at the expense of smaller ones. High-temperature-synthesized ( $T > 250$  °C) trioctylphosphine oxide (TOPO)/trioctyl phosphine (TOP)-capped CdSe quantum dots (QDs) (with Wurtzite (WZ)-type crystal structure<sup>9,10</sup>) were first surface-exchanged with 3-amino-1-propanol (APOL) to form APOL-capped CdSe QDs.<sup>9</sup> Following surface exchange, these NCs were annealed for various times at 135 °C in an APOL/H<sub>2</sub>O ( $v/v = 9/1$ ) mixture containing 0.1 M CdCl<sub>2</sub>. Figure S1 of the Supporting Information (SI) illustrates the UV–vis absorption of the NC solution as a function of annealing time, indicating both the depletion of the original NCs and the generation of larger- and smaller-sized NCs. The corresponding photoluminescence (PL) spectra (Figure S2 of the SI) are in agreement with the transformation of the original QDs (peaking at 582 nm) to smaller and larger NCs emitting at 446–506 and 585 nm, respectively. In accordance with our earlier reports,<sup>8,9</sup> the amine-assisted etching makes the smaller NCs considerably brighter than the larger ones. Subsequent surfactant exchange from APOL to TOPO/TOP/*n*-octylamine renders the large NCs insoluble in MeOH while the smaller NCs remain in the supernatant. Following a centrifugation step, the larger NCs were “recovered” as a precipitate and were redispersed in CHCl<sub>3</sub> for further characterization.

Figure 1a,b depicts the low- and high-magnification TEM images of the starting CdSe QDs. These NCs are elliptical in shape (average diameter and length of 4.4 and 6.7 nm, respectively) with aspect ratio of 1.6, as shown in Figure S3 of the SI. After 2 days of annealing at 135 °C, the majority of the “recovered” CdSe NCs were transformed to rods (with an average aspect ratio of 2.7), along with a few persisting dots, as shown in Figure 1c,d. HRTEM images of these rods (Figure 1d–h) indicates that these rods have one or two zinc blende (ZB) tips, which were not observed in the initial WZ CdSe QDs. The central part of the rods is populated mostly by a WZ-based structure, although the number of stacking faults along the *c*-axis has doubled to ca. 25%.

Figure 2a,b shows the UV–vis and PL emission of the starting and annealed CdSe NC samples, “recovered” from the annealing



**Figure 1.** Representative low- and high-magnification TEM images of CdSe NCs before (a,b) and after (c–f) annealing at 135 °C in 3-amino-1-propanol/H<sub>2</sub>O ( $v/v = 9/1$ ) with 0.1 M CdCl<sub>2</sub> for 48 h. Representative HRTEM images of rods (e–h) depict their zinc blende (ZB) tip(s) and stacking faults along the 002 axis. Scale bar = 2 nm.



**Figure 2.** Evolution of UV–vis absorption (a), PL emission (b), and PL fwhm (insets) of CdSe nanocrystals as a function of annealing time at 135 °C in APOL/H<sub>2</sub>O ( $v/v = 9/1$ ) with 0.1 M CdCl<sub>2</sub>.

solution. Progressively longer annealing times at 135 °C resulted in broadening of both the first electronic absorption and PL peaks relative to the original QD sample, indicated by the PL full width at half-maximum (fwhm) (Figure 2 inset). While the PL quantum yield of the starting and annealed solutions remained constant at ca. 10%, the PL peak red-shifted by ca. 3 nm and its fwhm increased from 40 to 49 nm.

<sup>†</sup> Institute of Materials Science.

<sup>‡</sup> Department of Chemistry.

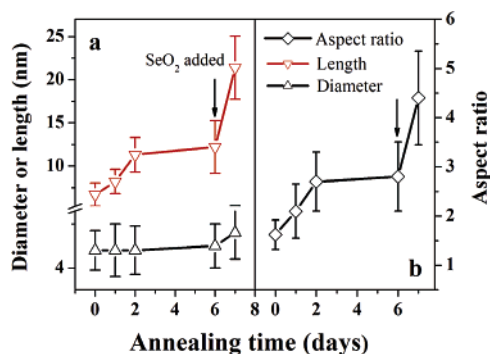


**Figure 3.** Evolution of length and diameter (a) as well as aspect ratio (b) of CdSe nanorods as a function of annealing time at 135 °C in APOL/H<sub>2</sub>O (v/v = 9/1) with 0.1 M CdCl<sub>2</sub>.

The gradual broadening of the PL spectra can be explained by the average diameter, length, and aspect ratio analysis shown in Figure 3a,b. During the first 2 days of annealing, the length of the NCs gradually increased from 6.7 to 11.4 nm, while their diameter remained almost the same. Further annealing for 4 more days produced no significant changes in both length and diameter. Earlier reports indicate that the starting crystal structure (WZ or ZB) of CdSe NCs is preserved during the amine-assisted etching process.<sup>8,9</sup> The gradual growth of NCs along the *c*-axis, together with the formation of ZB caps on the tips of these nanorods, provides a strong indication of a low-temperature growth process as opposed to an oriented NC attachment.<sup>11,12</sup> The attained equilibrium in rod growth along with the simultaneous production of progressively smaller NCs point toward an Ostwald ripening process.<sup>7,10</sup> If this is the case, the prevailing question is how Cd and Se ions are transferred from either the solution or smaller NCs to the growing end(s) of the rods.

A large excess of Cd<sup>2+</sup> ions within the annealing mixture was initially introduced to significantly slow the O<sub>2</sub>-induced CdSe NC etching.<sup>9</sup> Excess Cd<sup>2+</sup> ions could grow these rods, assuming that a Se source is present. Se, however, exists as Se<sup>2-</sup> ions that are strongly bound within the CdSe NCs. The elevated temperature stability of CdSe QDs in APOL/H<sub>2</sub>O mixtures (in the absence of O<sub>2</sub>) provides a strong indication that APOL-induced Se<sup>2-</sup> dissolution is highly unlikely.<sup>9</sup> However, in the presence of O<sub>2</sub>, selenium oxidation takes place to form SeO<sub>2</sub> that, due to its acidic character, is readily dissolved in the basic APOL.<sup>9</sup> Careful exclusion of O<sub>2</sub> (through repeated freeze–pump–thaw cycles) during this annealing process has shown no signs of dots-to-rods transformation, even after 6 days of annealing (Figures S4 and S5 of SI). This suggests that oxygen, through its formation of SeO<sub>2</sub>, plays a crucial role for such NC shape transformation. To verify this, following 6 days of regular annealing, 0.1 M SeO<sub>2</sub> was added and annealing was continued for 1 more day. The last point in Figure 3 indicates that, although there was a substantial increase in rod length and aspect ratio, the rod diameter grew to a lesser extent. Similarly, annealing of pure SeO<sub>2</sub> in APOL/H<sub>2</sub>O (v/v = 9/1) mixtures at 135 °C revealed that SeO<sub>2</sub> was reduced to Se<sup>0</sup>, as verified by X-ray photoelectron spectroscopy (XPS) and X-ray diffraction (XRD) characterization in Figures S6–S8 of the SI. Such redox behavior is believed to originate from amines that are capable of reducing SeO<sub>2</sub> to Se<sup>0</sup>. The reduction of CdTe and CdSe NCs to Te and Se nanowires, respectively, has been also reported recently in amine (EDTA) solutions.<sup>13</sup>

Figure S9 of the SI indicates that APOL is capable of dissolving Se<sup>0</sup>. The disproportionation of Se<sup>0</sup> to Se<sup>2-</sup> and SeO<sub>3</sub><sup>2-</sup> in basic environment provides the Se source for further growth at the expense of smaller CdSe NCs.<sup>14</sup> While this explains the low-temperature growth of the ZB caps, it leaves unanswered the question of why the rod diameter remains constant. Such asymmetric growth along the *c*-axis might originate from (i) the higher binding energy of water and/or amine surfactants to the rod side walls (i.e., {01 $\bar{1}$ 0} and {11 $\bar{2}$ 0}) as opposed to the propagating ends;<sup>15</sup> (ii) the 1:1 Cd:Se stoichiometry of side walls, stabilizing the respective oxide as opposed to the propagating Cd- or Se-terminated ends;<sup>8,9</sup> or (iii) the progressively higher etching rate of non-closed-shell structures that might nucleate on the side walls of the rods,<sup>8,9</sup> which maintains a constant rod diameter. Further investigations are currently underway to identify the underlying mechanism responsible for such asymmetric growth.

In conclusion, the low-temperature annealing of CdSe NCs in APOL/H<sub>2</sub>O mixtures in the presence of oxygen and CdCl<sub>2</sub> has led to the asymmetric growth of larger NCs at the expense of smaller ones. This growth takes place along the *c*-axis, while the original diameter is maintained. Such dots-to-rod transformation, in combination with the preferential etching of various crystalline planes,<sup>9</sup> might find a variety of applications in the fabrication of specialized semiconductor nanostructures and their devices.

**Acknowledgment.** The authors thank Prof. M. Aindow, Dr. J. Gromek, Dr. D. Goberman, and Mr. J. Doll for helpful discussions. Financial support from ONR, ARO, and NSF is greatly appreciated.

**Supporting Information Available:** Experimental details and UV–vis, PL, XPS, XRD, TEM, and size analyses. This material is available free of charge via the Internet at <http://pubs.acs.org>.

## References

- (1) (a) Alivisatos, A. P. *J. Phys. Chem.* **1996**, *100*, 13226–13239. (b) Murray, C. B.; Kagan, C. R.; Bawendi, M. G. *Annu. Rev. Mater. Sci.* **2000**, *30*, 545–610.
- (2) Manna, L.; Scher, E. C.; Alivisatos, A. P. *J. Cluster Sci.* **2002**, *13*, 521–532.
- (3) Peng, X. *Adv. Mater.* **2003**, *15*, 459–463.
- (4) (a) Hu, J.; Li, L.-s.; Yang, W.; Mana, L.; Wang, L.-w.; Alivisatos, A. P. *Science* **2001**, *292*, 2060–2063. (b) Chen, X.; Nazzari, A.; Gooskey, D.; Xiao, M.; Peng, Z. A.; Peng, X. *Phys. Rev. B* **2001**, *64*, 245304/1–245304/4.
- (5) Peng, X. G.; Manna, L.; Yang, W. D.; Wickham, J.; Scher, E.; Kadavanich, A.; Alivisatos, A. P. *Nature* **2000**, *404*, 59–61.
- (6) Nair, P. S.; Fritz, K. P.; Scholes, G. D. *Chem. Commun. (Cambridge, U.K.)* **2004**, 2084–2085.
- (7) Peng, Z. A.; Peng, X. *J. Am. Chem. Soc.* **2001**, *123*, 1389–1395.
- (8) Li, R.; Lee, J.; Kang, D.; Luo, Z.; Aindow, M.; Papadimitrakopoulos, F. *Adv. Funct. Mater.* **2006**, 345–350.
- (9) Li, R.; Lee, J.; Yang, B.; Horspool, D. N.; Aindow, M.; Papadimitrakopoulos, F. *J. Am. Chem. Soc.* **2005**, *127*, 2524–2532.
- (10) Murray, C. B.; Norris, D. J.; Bawendi, M. G. *J. Am. Chem. Soc.* **1993**, *115*, 8706–8715.
- (11) Pacholski, C.; Kornowski, A.; Weller, H. *Angew. Chem., Int. Ed.* **2002**, *41*, 1188–1191.
- (12) Tang, Z.; Kotov, N. A.; Giersig, M. *Science* **2002**, *297*, 237–240.
- (13) Tang, Z.; Wang, Y.; Sun, K.; Kotov, N. A. *Adv. Mater.* **2005**, *17*, 358–363.
- (14) Talapin, D. V.; Rogach, A. L.; Shevchenko, E. V.; Kornowski, A.; Haase, M.; Weller, H. *J. Am. Chem. Soc.* **2002**, *124*, 5782–5790.
- (15) Puzder, A.; Williamson, A. J.; Zaitseva, N.; Galli, G.; Manna, L.; Alivisatos, A. P. *Nano Lett.* **2004**, *4*, 2361–2365.

JA058102I